Los Alamos
NATIONAL LABORATORY
EST. 1943

LA-UR-20-23257
Approved for public release; distribution is unlimited.

Title: Stress from long-range interactions in particulate system

Author(s): Zhang, Duan Zhong

Intended for: Report

Issued: 2020-04-29

Disclaimer:
Los Alamos National Laboratory, an affirmative action/equal opportunity employer, is operated by Triad National Security, LLC for the National Nuclear Security Administration of U.S. Department of Energy under contract 89233218CNA000001. By approving this article, the publisher recognizes that the U.S. Government retains nonexclusive, royalty-free license to publish or reproduce the published form of this contribution, or to allow others to do so, for U.S. Government purposes. Los Alamos National Laboratory requests that the publisher identify this article as work performed under the auspices of the U.S. Department of Energy. Los Alamos National Laboratory strongly supports academic freedom and a researcher's right to publish; as an institution, however, the Laboratory does not endorse the viewpoint of a publication or guarantee its technical correctness.

Stress from long-range interactions in particulate system

Duan Z. Zhang[1, a)]
Fluid Dynamics and Solid Mechanics Group, T–3, Theoretical Division, Los Alamos National Laboratory, Los Alamos, NM 87545, USA

(Dated: 23 April 2020)

In particulate systems, the ensemble average accounting for effects from all particles is expressed as the expected value related to the nearest particle probability. Using this expression, a stress is defined even for long-range particle interactions without the divergence difficulty because of the rapid far field decay of the probability. Similar to the potential part of the virial stress in molecular systems, this stress represents particle-particle interactions through the surrounding field. As examples, the stresses are calculated for systems of charged particles and disperse multiphase flows.

I. INTRODUCTION

Long-range particle interactions have been difficult to study in many fields of physics, especially for the closure relations of the averaged equations for multiphase flows. Numerical simulations for these particulate systems mostly rely on the Ewald sum technique.[1–4] To numerically study long-range particle-fluid-particle or particle-field-particle (PFP) interactions, one inevitably has to involve the computational domain size, hampering direct analysis of the effects of gradients in the system. As a result, most numerical simulations[2,3,5–7] are limited to uniform systems.

The main objective of this work is to show that there is a screening effect related to the inter-particle length scale and that a PFP stress can be rigorously defined for particulate systems, when the concept of the average conditional on the nearest particle is used. This screening is different from the Brinkman screening[8] in Stokes flows or Debye screening[9] in charge neutral systems in thermodynamic equilibrium. While the nearest particle is an old concept,[10] the starting point of this work is a new relation derived in the next section between the ensemble average and the average conditional on the nearest particle. This relation accounts for not only the pair interaction between the nearest neighbors, but also effects from all other particles, while bypassing the difficulty of divergent integrals in the study of long-range PFP interactions. This relation and the PFP stress definition are valid for general particulate systems, such as colloidal suspensions, charged dust clouds, and galaxies with gravitational effects.

From the point of view of the fundamental physics, the momentum equation is a consequence of spatial symmetry, or invariance under spatial translation. Stresses are parts of the Noether current. The spatial translation at each length scale reveals a stress. The spatial translation at the inter-molecular length scale reveals the potential part of the virial stress.[11] In particulate systems, there are two important length scales, the particle size and the inter-particle distance. The spatial translation at the length scale of the particle size leads to the stresses caused by intra- and inter-phase interactions.[12–14] In this work, the PFP stress is found by a spatial translation at the length scale of the inter-particle distance as shown in Section 3 using the newly derived relation between the ensemble average and the nearest particle statistics in the next section.

As examples in Section 4, particulate systems are studied using the nearest particle statistics developed in this work. The PFP pressure from Coulomb interactions of charged particles is calculated. To show the relation between this method and the Debye screening, the Debye-Hückel equation is derived. A more important application of this method is the calculation of the PFP stresses in disperse multiphase flows, which has a significant consequence for the multiphase flow theory as discussed in the section.

II. NEAREST PARTICLE STATISTICS AND ENSEMBLE AVERAGE

Let $\mathscr{C}$, called configuration, be a set of parameters uniquely describing a particulate system, and $P(\mathscr{C})$ be the probability density of configuration $\mathscr{C}$ at time t. In this work, only spatial variations are of concern; therefore, we suppress variable t in all the functions, while the results are applicable to time varying systems. The particle number density $n_p(\boldsymbol{x})$ at location $\boldsymbol{x}$ is defined as[11,12,14–16]

$$n_p(\boldsymbol{x}) = \int \sum_i \delta(\boldsymbol{x} - \boldsymbol{\xi}_i) P(\mathscr{C}) d\mathscr{C}, \tag{1}$$

where the summation is over all particles in the configuration, and $\boldsymbol{\xi}_i$ is the position of particle i. Similarly, the

a)Electronic mail: dzhang@lanl.gov

pair distribution function $P_2(\boldsymbol{x},\boldsymbol{y})$ is defined as

$$P_2(\boldsymbol{x},\boldsymbol{y}) = \int \sum_i \sum_{j\neq i} \delta(\boldsymbol{x}-\boldsymbol{\xi}_i)\delta(\boldsymbol{y}-\boldsymbol{\xi}_j)P(\mathscr{C})d\mathscr{C}. \quad (2)$$

For a generic particle quantity g, let $g_i(\mathscr{C})$ be its value on particle i in configuration $\mathscr{C}$. The ensemble average of this quantity at location $\boldsymbol{x}$ is[11,12,14–16]

$$\overline{g}(\boldsymbol{x}) = \frac{1}{n_p(\boldsymbol{x})}\int \sum_i \delta(\boldsymbol{x}-\boldsymbol{\xi}_i)g_i(\mathscr{C})P(\mathscr{C})d\mathscr{C}. \quad (3)$$

To relate the ensemble average to the nearest particle statistics, we introduce a function

$$h_{ij}(\mathscr{C}) = \frac{1}{N_i}\prod_{k\neq i,k\neq j} H(|\boldsymbol{\xi}_k-\boldsymbol{\xi}_i|-|\boldsymbol{\xi}_j-\boldsymbol{\xi}_i|), \quad (4)$$

where the product is over all particles in the configuration, H is the Heaviside function (with the convention $H(0)=1$), N_i is the number of the nearest particles to particle i, which are at the equal distance away from particle i. The function $h_{ij}(\mathscr{C}) = 1/N_i$, if particle j is one of the nearest neighbors to particle i in configuration $\mathscr{C}$; and $h_{ij}(\mathscr{C}) = 0$ otherwise.

Using the property of the δ-function, for any configuration $\mathscr{C}$ and any particle, say i, one has,

$$\int \sum_{j\neq i}\delta(\boldsymbol{y}-\boldsymbol{\xi}_j)h_{ij}(\mathscr{C})d^3y = \sum_{j\neq i} h_{ij}(\mathscr{C}) = 1. \quad (5)$$

The last equality comes from the fact that the summation over all the particles (j's) in a configuration encounters all the nearest particles of particle i. Multiplying the left-hand side of (5), which is 1, to the right-hand side of (3) and then exchanging the orders of the integrations, one finds a major relation of this work relating the ensemble average to the nearest particle statistics,

$$n_p(\boldsymbol{x})\overline{g}(\boldsymbol{x}) = \int \overline{g}_{nst}(\boldsymbol{x},\boldsymbol{y})\overline{h}_2(\boldsymbol{x},\boldsymbol{y})P_2(\boldsymbol{x},\boldsymbol{y})d^3y, \quad (6)$$

where

$$\overline{g}_{nst}(\boldsymbol{x},\boldsymbol{y}) = \frac{1}{\overline{h}_2(\boldsymbol{x},\boldsymbol{y})P_2(\boldsymbol{x},\boldsymbol{y})}\int \sum_i \delta(\boldsymbol{x}-\boldsymbol{\xi}_i)g_i(\mathscr{C}) \sum_{j\neq i}\delta(\boldsymbol{y}-\boldsymbol{\xi}_j)h_{ij}(\mathscr{C})P(\mathscr{C})d\mathscr{C}, \quad (7)$$

with $\overline{h}_2(\boldsymbol{x},\boldsymbol{y})$ chosen to be

$$\overline{h}_2(\boldsymbol{x},\boldsymbol{y}) = \frac{1}{P_2(\boldsymbol{x},\boldsymbol{y})}\int \sum_i \delta(\boldsymbol{x}-\boldsymbol{\xi}_i) \sum_{j\neq i}\delta(\boldsymbol{y}-\boldsymbol{\xi}_j)h_{ij}(\mathscr{C})P(\mathscr{C})d\mathscr{C}, \quad (8)$$

such that $\overline{g}_{nst}(\boldsymbol{x},\boldsymbol{y}) = 1$, when $g_i(\mathscr{C}) = 1$.

In definitions (7) and (8), the two δ-functions on the right-hand sides ensure that the contributions to the integrals only come from the configurations in which positions $\boldsymbol{x}$ and $\boldsymbol{y}$ are occupied by a pair of particles. Function $h_{ij}(\mathscr{C})$ further restricts that the contributions are only from the configurations in which the particle at $\boldsymbol{y}$ is one of the nearest neighbors to the particle at $\boldsymbol{x}$. After division by P_2, $\overline{h}_2$ defined in (8) is the probability of the particle at $\boldsymbol{y}$ being the nearest neighbor to the particle at $\boldsymbol{x}$, given a particle pair at positions $\boldsymbol{x}$ and $\boldsymbol{y}$.

Similarly, $\overline{g}_{nst}(\boldsymbol{x},\boldsymbol{y})$ defined in (7) is the average of particle quantity g at $\boldsymbol{x}$, under the condition that $\boldsymbol{y}$ is occupied by one of the nearest particles to the particle at $\boldsymbol{x}$. The quantity $g_i(\mathscr{C})$ in (7) is the value of g on particle i, including effects from all particles in configuration $\mathscr{C}$.

Multiplying (8) by $P_2(\boldsymbol{x},\boldsymbol{y})$, then integrating over $\boldsymbol{y}$, after using (5) and (1), one finds

$$\int \overline{h}_2(\boldsymbol{x},\boldsymbol{y})P_2(\boldsymbol{x},\boldsymbol{y})d^3y = n_p(\boldsymbol{x}). \quad (9)$$

This relation implies that the integral in (6) over the entire space converges absolutely for any bounded function $\overline{g}_{nst}(\boldsymbol{x},\boldsymbol{y})$, even it results from long-range PFP interactions. Moreover, $\overline{h}_2$ decays as $\exp(-4\pi n_p|\boldsymbol{y}-\boldsymbol{x}|^3/3)$ at a large distance between the pair of particles in many common cases;[10,17–19] therefore, using the quantity averaged conditionally on the nearest particle, we are free of the difficulty of divergent integrals often encountered[1,3,15,20] in studies of long-range particle interactions. Although the mathematical derivations above add no new physics and do not alter the long-range nature of the particle interactions, the convergence of (6) facilitates further mathematical derivations to examine the physics in the system. One example is the study of the PFP interactions at the length scale of the inter-particle distance, resulting in the concept of the PFP stress as shown below.

III. PARTICLE-FIELD-PARTICLE STRESS

Let $\overline{\boldsymbol{f}}_{nst}(\boldsymbol{x},\boldsymbol{y})$ be the average particle-field interaction force on the particle at $\boldsymbol{x}$ conditional on the nearest particle at $\boldsymbol{y}$ defined using (7) with $g_i(\mathscr{C}) = \boldsymbol{f}_{pf,i}(\mathscr{C})$, which is the force on particle i applied by its surrounding field containing effects from all particles in the configuration. According to (6), the ensemble average of the particle-field interaction force on a particle at $\boldsymbol{x}$ is

$$\overline{\boldsymbol{f}}_{pf}(\boldsymbol{x}) = \frac{1}{n_p(\boldsymbol{x})}\int \boldsymbol{F}(\boldsymbol{x},\boldsymbol{r})d^3r, \quad (10)$$

where $\boldsymbol{r} = \boldsymbol{y}-\boldsymbol{x}$, and

$$\boldsymbol{F}(\boldsymbol{x},\boldsymbol{r}) = \overline{\boldsymbol{f}}_{nst}(\boldsymbol{x},\boldsymbol{y})\overline{h}_2(\boldsymbol{x},\boldsymbol{y})P_2(\boldsymbol{x},\boldsymbol{y}), \quad (11)$$

is the force density in the six-dimensional $(\boldsymbol{x},\boldsymbol{r})$ space. The probable force

$$\boldsymbol{f}_{eb}(\boldsymbol{x},\boldsymbol{y}) = \overline{\boldsymbol{f}}_{nst}(\boldsymbol{x},\boldsymbol{y})\overline{h}_2(\boldsymbol{x},\boldsymbol{y}) \tag{12}$$

can be considered as the effective binary interaction force applied by the particle at $\boldsymbol{y}$ to the particle at $\boldsymbol{x}$, if the presence of the surrounding field is not explicitly considered. This force contains both particle-particle and particle-mean field (although not explicitly considered) interactions and is similar to the Coulomb force between a pair of charged particles. Rigorously speaking, the charged particles only interact with the surrounding field, not directly with each other, but when the electromagnetic waves caused by motion of the particles are negligible, one can directly use the Coulomb law to calculate the forces between them without considering the field explicitly.

To explore PFP interactions, we introduce the k-th order moment,

$$\boldsymbol{S}_k(\boldsymbol{x}) = \frac{1}{k!}\int \boldsymbol{r}^k \boldsymbol{F}(\boldsymbol{x},\boldsymbol{r})d^3r, \tag{13}$$

where $\boldsymbol{r}^k$ denotes the dyadic product of k $\boldsymbol{r}$'s and is a k-th order tensor, and $\boldsymbol{S}_k$ is a $(k+1)$-th order tensor. These moments contain information about PFP interactions at the inter-particle length scale ℓ_p.

With the change of integration variable $\boldsymbol{r} = -\boldsymbol{r}'$, for an integer $k \geq 0$, one finds

$$\int \boldsymbol{r}^k \boldsymbol{F}(\boldsymbol{x},\boldsymbol{r})d^3r = (-1)^k \int \boldsymbol{r}^k \boldsymbol{F}(\boldsymbol{x},-\boldsymbol{r})d^3r. \tag{14}$$

Using this relation for $k = 0$, we can rewrite (10) as

$$n_p(\boldsymbol{x})\overline{\boldsymbol{f}}_{pf}(\boldsymbol{x}) = \frac{1}{2}\int [\boldsymbol{F}(\boldsymbol{x},\boldsymbol{r}) + \boldsymbol{F}(\boldsymbol{x},-\boldsymbol{r})]d^3r. \tag{15}$$

The first variable of $\boldsymbol{F}(\boldsymbol{x},\boldsymbol{r})$ is the location of the particle subjected to the force. The length scale associated with this variable is the length scale L of the physical problem. The second variable $\boldsymbol{r}$ represents the variation at the inter-particle length scale ℓ_p. For problems that averaged equations are applicable, $L >> \ell_p$. Compared to $\boldsymbol{r}$, $\boldsymbol{x}$ is a slowly varying variable[21] for $\boldsymbol{F}(\boldsymbol{x},\boldsymbol{r})$. To study PFP interactions, we consider forces on different particles using the Taylor series on the slowly varying variable $\boldsymbol{x}$.

$$\boldsymbol{F}\Big(\boldsymbol{x} \mp \frac{\boldsymbol{r}}{2}, \pm\boldsymbol{r}\Big) = \boldsymbol{F}(\boldsymbol{x},\pm\boldsymbol{r}) + \sum_{k=1}^{\infty}\frac{1}{k!}\Big(\frac{\mp\boldsymbol{r}}{2}\Big)^k : \nabla_x^k \boldsymbol{F}(\boldsymbol{x},\pm\boldsymbol{r}), \tag{16}$$

where the subscript x in ∇_x denotes that the gradient operator only acts on the first (slowly varying) variable $\boldsymbol{x}$, ∇_x^k denotes the dyadic product of k ∇_x's and is a k-th order tensor operator, and $\boldsymbol{r}^k : \nabla_x^k \boldsymbol{F}$ denotes the inner product between $\boldsymbol{r}^k$ and $\nabla_x^k \boldsymbol{F}$.

Using (16) in (15), and then (14), one finds

$$n_p(\boldsymbol{x})\overline{\boldsymbol{f}}_{pf}(\boldsymbol{x}) = n_p(\boldsymbol{x})\boldsymbol{f}_o(\boldsymbol{x}) - \nabla_x \cdot \Big[\sum_{k=1}^{\infty}\frac{(-1)^k}{2^k}\nabla_x^{k-1} : \boldsymbol{S}_k\Big], \tag{17}$$

where

$$n_p(\boldsymbol{x})\boldsymbol{f}_o(\boldsymbol{x}) = \int \frac{\boldsymbol{F}\big(\boldsymbol{x}-\frac{\boldsymbol{r}}{2},\boldsymbol{r}\big) + \boldsymbol{F}\big(\boldsymbol{x}+\frac{\boldsymbol{r}}{2},-\boldsymbol{r}\big)}{2}d^3r. \tag{18}$$

In the second term on the right-hand side of (17), the orders of the integration and the gradient operators have been exchanged. This is legitimate because ∇_x acts on $\boldsymbol{x}$, while the integration variable is $\boldsymbol{r}$. The quantity inside the square brackets is a tensor with the dimension of stress, but it is not a stress. To see that, let us decompose $\boldsymbol{F}$ into the symmetric part,

$$\boldsymbol{F}_s(\boldsymbol{x},\boldsymbol{r}) = \frac{1}{2}[\boldsymbol{F}(\boldsymbol{x},\boldsymbol{r}) + \boldsymbol{F}(\boldsymbol{x},-\boldsymbol{r})], \tag{19}$$

representing the pair-field interaction at position $\boldsymbol{x}$, and the antisymmetric part,

$$\boldsymbol{F}_a(\boldsymbol{x},\boldsymbol{r}) = \frac{1}{2}[\boldsymbol{F}(\boldsymbol{x},\boldsymbol{r}) - \boldsymbol{F}(\boldsymbol{x},-\boldsymbol{r})], \tag{20}$$

representing the PFP interaction at the position. Clearly,

$$\boldsymbol{F}_s(\boldsymbol{x},\boldsymbol{r}) = \boldsymbol{F}_s(\boldsymbol{x},-\boldsymbol{r}), \quad \boldsymbol{F}_a(\boldsymbol{x},\boldsymbol{r}) = -\boldsymbol{F}_a(\boldsymbol{x},-\boldsymbol{r}). \tag{21}$$

Since a stress represents force transmission through a surface, let us consider surface element dA between particles at $\boldsymbol{x}$ and $\boldsymbol{x}+\boldsymbol{r}$ with unit normal $\hat{\boldsymbol{r}} = \boldsymbol{r}/r$. The force caused by a stress, say $\boldsymbol{\sigma}$, on the surface element is $\boldsymbol{\sigma}\cdot\hat{\boldsymbol{r}}dA$, which changes its sign when the distance vector $\boldsymbol{r}$ between the particles does. If a force component between the pair contributes to a stress, the force component must also change its sign. Hence, only the antisymmetric part $\boldsymbol{F}_a$ of $\boldsymbol{F}$ can contribute to a stress. Using (14) or (21), one can show that the antisymmetric part $\boldsymbol{F}_a$ contributes to and only to $\boldsymbol{S}_k$ with odd k's; and the symmetric part $\boldsymbol{F}_s$ contributes to and only to $\boldsymbol{S}_k$ with even k's. With these properties of $\boldsymbol{S}_k$, we now define the PFP stress $\boldsymbol{\Sigma}_{pfp}$ as

$$\theta_p(\boldsymbol{x})\boldsymbol{\Sigma}_{pfp}(\boldsymbol{x}) = \sum_{odd\,k>0}^{\infty}\frac{1}{2^k}\nabla^{k-1} : \boldsymbol{S}_k(\boldsymbol{x}), \tag{22}$$

and the pseudo-stress $\boldsymbol{T}$ as

$$\theta_p(\boldsymbol{x})\boldsymbol{T}(\boldsymbol{x}) = \sum_{even\,k>0}^{\infty}\frac{1}{2^k}\nabla^{k-1} : \boldsymbol{S}_k(\boldsymbol{x}). \tag{23}$$

The volume fraction θ_p is multiplied with $\boldsymbol{\Sigma}_{pfp}$ and $\boldsymbol{T}$ in these definitions to serve as a reminder that $\theta_p\boldsymbol{\Sigma}_{pfp}$ and $\theta_p\boldsymbol{T}$ go to zero as the particle volume fraction θ_p does, although not necessarily linearly with θ_p.

With these definitions, the particle-field interaction force density becomes

$$n_p(\boldsymbol{x})\boldsymbol{f}_{pf}(\boldsymbol{x})=n_p(\boldsymbol{x})\boldsymbol{f}_\ell(\boldsymbol{x})+\nabla\cdot[\theta_p(\boldsymbol{x})\boldsymbol{\Sigma}_{pfp}(\boldsymbol{x})], \quad (24)$$

where $\boldsymbol{f}_\ell$ is the local force defined as

$$n_p(\boldsymbol{x})\boldsymbol{f}_\ell(\boldsymbol{x})=n_p(\boldsymbol{x})\boldsymbol{f}_o(\boldsymbol{x})-\nabla\cdot[\theta_p(\boldsymbol{x})\boldsymbol{T}(\boldsymbol{x})]. \quad (25)$$

To understand the physical meaning of $\boldsymbol{f}_\ell$, let us focus on the first term, since the second term is of order $(\ell_p/L)^2$. Using (11) and property $P_2(\boldsymbol{x},\boldsymbol{y}) = P_2(\boldsymbol{y},\boldsymbol{x})$ from definition (2), we rewrite (18) as

$$n_p(\boldsymbol{x})\boldsymbol{f}_o(\boldsymbol{x})=\int \boldsymbol{f}_{pr}(\boldsymbol{x},\boldsymbol{r})P_2\big(\boldsymbol{x}-\frac{\boldsymbol{r}}{2},\boldsymbol{x}+\frac{\boldsymbol{r}}{2}\big)d^3r, \quad (26)$$

where

$$\boldsymbol{f}_{pr}(\boldsymbol{x},\boldsymbol{r})=\frac{1}{2}\Big[\boldsymbol{f}_{eb}\big(\boldsymbol{x}-\frac{\boldsymbol{r}}{2},\boldsymbol{x}+\frac{\boldsymbol{r}}{2}\big)+\boldsymbol{f}_{eb}\big(\boldsymbol{x}+\frac{\boldsymbol{r}}{2},\boldsymbol{x}-\frac{\boldsymbol{r}}{2}\big)\Big]. \quad (27)$$

The first term in (27) is the effective binary force on the particle at $\boldsymbol{x}-\frac{\boldsymbol{r}}{2}$ from the particle at $\boldsymbol{x}+\frac{\boldsymbol{r}}{2}$; and the second term is the force the other way around. The force $\boldsymbol{f}_{pr}$ in (27) represents the average force per particle due to the interaction between the pair and the surrounding field. After integrating over all particle pairs around $\boldsymbol{x}$, force $\boldsymbol{f}_o$ is the average pair-field interaction force per particle. However, the force $\boldsymbol{f}_{pr}$ is on particles at $\boldsymbol{x}\pm\boldsymbol{r}/2$, not on a particle at $\boldsymbol{x}$. The effect of this position difference to the local force $\boldsymbol{f}_\ell$ is of order $(\ell_p/L)^2$ and is corrected by the subtraction of the pseudo-stress in (25), which only involves the symmetric part of $\boldsymbol{F}(\boldsymbol{x},\boldsymbol{r})$, representing the pair-field interaction at the location.

Such calculated $\boldsymbol{f}_\ell(\boldsymbol{x})$ is the pair-field force per particle at $\boldsymbol{x}$. The total particle-field force $\boldsymbol{f}_{pf}$ on a single particle at $\boldsymbol{x}$ needs to include intra-pair interactions, which is the divergence of the PFP stress. To illustrate the physical meaning of the PFP stress, we only consider the first term, $\boldsymbol{S}_1$ in (22).

Let dA be a surface element centered at $\boldsymbol{x}$ with the unit normal $\boldsymbol{n}$ as shown in Fig. 1. For a given distance vector $\boldsymbol{r}$, inside the cylinder are the locations ($\boldsymbol{z}$'s) of particles, such that another particle at distance $\boldsymbol{r}$ away from a particle (at $\boldsymbol{z}$) in the cylinder is on the other side of (above) the surface element dA. The volume of the cylinder is $dV_z = \boldsymbol{n}\cdot\boldsymbol{r}dA$. The cylinder contains $n_p\boldsymbol{n}\cdot\boldsymbol{r}dA$ probable particles. The probable number of particle pairs with a particle in the cylinder, and the other particle in the volume element d^3r at distance $\boldsymbol{r}$ away from the particle at $\boldsymbol{z}$ in the cylinder is $\boldsymbol{n}\cdot\boldsymbol{r}dAP_2(\boldsymbol{z},\boldsymbol{z}+\boldsymbol{r})d^3r$.

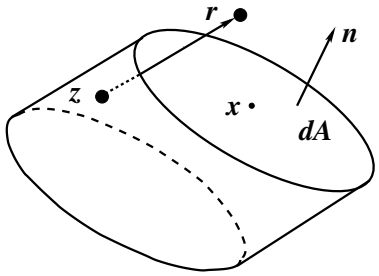

FIG. 1. Illustration of PFP interactions across a surface element dA containing $\boldsymbol{x}$. For a given vector $\boldsymbol{r}$, the cylinder is constructed to have its side parallel to $\boldsymbol{r}$ with length r.

Particles in these pairs are on the different sides of the surface element dA. Each such pair transmits a probable force $\boldsymbol{f}_{eb}(\boldsymbol{z},\boldsymbol{z}+\boldsymbol{r})$ across the surface element dA. By noting $\boldsymbol{F}(\boldsymbol{z},\boldsymbol{r}) = \boldsymbol{f}_{eb}(\boldsymbol{z},\boldsymbol{z}+\boldsymbol{r})P_2(\boldsymbol{z},\boldsymbol{z}+\boldsymbol{r})$ from (11) and (12), after integrating over all such cylinders represented by $\boldsymbol{r}$'s, the integral

$$\boldsymbol{\tau}dA = dA\boldsymbol{n}\cdot\int_{\boldsymbol{n}\cdot\boldsymbol{r}>0}\boldsymbol{r}\boldsymbol{F}(\boldsymbol{z},\boldsymbol{r})d^3r \quad (28)$$

is the total effective particle interaction force applied across the surface area dA by the particles on the positive ($\boldsymbol{n}\cdot\boldsymbol{r}>0$, above the plane) side to the particles on the negative side ($\boldsymbol{n}\cdot\boldsymbol{r}<0$) of the surface element dA, and $\boldsymbol{\tau}$ is the traction force per unit area. Similar calculations can be performed for the particle forces in the reverse direction to yield the same expression as (28), but with the integration region changed to $\boldsymbol{n}\cdot\boldsymbol{r}<0$. Combining these results from both sides, within an error of $O(\ell_p/L)^2$ on the stress, resulting an $O(\ell_p/L)^3$ error on the force as in (24), one can approximate $\boldsymbol{z}$ with $\boldsymbol{x}$ and finds $\boldsymbol{\tau}dA = dA\boldsymbol{n}\cdot[\theta_p(\boldsymbol{x})\boldsymbol{\Sigma}_{pfp}(\boldsymbol{x})]$, with $\theta_p(\boldsymbol{x})\boldsymbol{\Sigma}_{pfp}(\boldsymbol{x})$ calculated in (22).

IV. EXAMPLES

We now use examples to show calculations of this PFP stress and applications of the nearest particle statistics.

A. Systems with electric charges

Let us consider a system of charged spherical particles. Each particle contains the same amount of charge q and has a radius a. For a particle at $\boldsymbol{x}$, the force on the particle conditional on the nearest particle at $\boldsymbol{y}$ is

$$\overline{\boldsymbol{f}}_{nst}(\boldsymbol{x},\boldsymbol{y}) = -\frac{q^2}{4\pi\varepsilon r^2}\hat{\boldsymbol{r}} + q\boldsymbol{E}_0(\boldsymbol{x}) \quad (29)$$

where ε is the electric permittivity, $\boldsymbol{r} = \boldsymbol{y} - \boldsymbol{x}$ is the distance vector between the particles, $\hat{\boldsymbol{r}} = \boldsymbol{r}/r$, and $\boldsymbol{E}_0(\boldsymbol{x})$ is the electric field at $\boldsymbol{x}$ if the particle at $\boldsymbol{y}$ is absent. The particle-field-particle stress defined in (22) can be calculated as

$$\theta_p \boldsymbol{\Sigma}_{pfp} = \frac{1}{2}\int \boldsymbol{r}\overline{\boldsymbol{f}}_{nst}\overline{h}_2 P_2 d^3r = -\int \frac{q^2}{8\pi\varepsilon r}\hat{\boldsymbol{r}}\hat{\boldsymbol{r}}\overline{h}_2 P_2 d^3r, \quad (30)$$

because the second term in (29) integrates to zero. This integral converges for any particle distribution as discussed above. By assuming uniform and isotropic particle distribution and a small particle volume fraction, we have[15,18,19] $\overline{h}_2 \approx \exp[-4\pi n_p(r^3 - (2a)^3)/3]$ and $P_2 \approx n_p^2$. The integration can be performed analytically to find

$$\theta_p \boldsymbol{\Sigma}_{pfp} \approx -\frac{\rho^2 a^2 \theta_p^{4/3}}{18\varepsilon} e^{8\theta_p}\Gamma_{inc}\left(\frac{2}{3}, 8\theta_p\right)\boldsymbol{I}, \quad (31)$$

where $\rho = q/(4\pi a^3/3)$ is the average charge density in the particle, Γ_{inc} is the incomplete Γ-function, and $\boldsymbol{I}$ is the identity tensor. This stress is negative indicating the pressure in the system causing the tendency of expansion.

To show the relationship between the nearest particle statistics and the Debye screening, we consider a system containing N species of charged point particles subjected to a weak electric potential $\phi << k_bT/q$, where k_b is the Boltzmann constant, T is the absolute temperature, and q is the typical charge on a particle. The system is otherwise statistically homogeneous and isotropic.

For multi-species systems, we apply the nearest particle statistics to one of the species, say species, s. Since the electric field $\boldsymbol{E}$ is not a particle quantity, but defined everywhere in space, relation (6) cannot be used directly. A similar relation (eq. (56) in the Appendix) for the continuous phase quantities can be derived. The ensemble average of $\boldsymbol{E}$ can be written as

$$\langle \boldsymbol{E}\rangle(\boldsymbol{x}) = \int \langle \boldsymbol{E}\rangle_{s,nst}(\boldsymbol{x},\boldsymbol{r}) P^c_{s,nst}(\boldsymbol{x},\boldsymbol{r}) d^3r, \quad (32)$$

where $P^c_{s,nst}(\boldsymbol{x},\boldsymbol{r})$ ($= P^c_{nst}(\boldsymbol{x}+\boldsymbol{r}|\boldsymbol{x})$ in (56)) is the probability density of finding the nearest species s particle to $\boldsymbol{x}$ at $\boldsymbol{x}+\boldsymbol{r}$, and $\langle \boldsymbol{E}\rangle_{s,nst}(\boldsymbol{x},\boldsymbol{r})$ ($= \langle q_c\rangle_{nst}(\boldsymbol{x},\boldsymbol{x}+\boldsymbol{r})$ in (56)) is the averaged electric field at $\boldsymbol{x}$ conditional on the nearest species s particle at the distance $\boldsymbol{r}$ away. After applying the Gauss law (by using (60) in the Appendix with $q_c = \boldsymbol{E}$ and $\chi_c = \theta_c = 1$, noting the homogeneity of the system, and neglecting the last term representing multi-particle interactions), correct to the first order in the species concentration,[22] we have

$$\varepsilon\nabla\cdot\langle \boldsymbol{E}\rangle_{s,nst}(\boldsymbol{x},\boldsymbol{r}) = \sum_{k=1}^{N} q_k n^k_{s,nst}(\boldsymbol{x},\boldsymbol{r}), \quad (33)$$

where $n^k_{s,nst}(\boldsymbol{x},\boldsymbol{r})$ is the number density of species k particles at $\boldsymbol{x}$, under the condition that the nearest species s particle at $\boldsymbol{x}+\boldsymbol{r}$.

Let $\langle\phi\rangle_{s,nst}$ be the potential for $\langle \boldsymbol{E}\rangle_{s,nst}$, such that $\langle \boldsymbol{E}\rangle_{s,nst} = -\nabla\langle\phi\rangle_{s,nst}$. Under the assumption of thermodynamic equilibrium and small electric potential $\phi << k_bT/q$, we have the Boltzmann distribution

$$n^k_{s,nst} = n^k_0 \exp\left(-\frac{q_k\langle\phi\rangle_{s,nst}}{k_bT}\right) \approx n^k_0\left(1 - \frac{q_k\langle\phi\rangle_{s,nst}}{k_bT}\right), \quad (34)$$

where n^k_0 is the mean number density of species k particles. Using this relation in (33) and noting $\sum_{k=1}^{N} n^k_0 q_k = 0$ for charge neutrality, one finds

$$\nabla^2\langle\phi\rangle_{s,nst} - \frac{\langle\phi\rangle_{s,nst}}{\ell_d^2} = 0, \quad (35)$$

where $\ell_d = \sqrt{\varepsilon k_bT/\sum_{i=1}^{N}(n_i^0 q_i^2)}$ is the Debye length. Equation (35) is known as the Debye-Hückel equation, which has a fundamental solution[22]

$$\langle\phi\rangle_{s,nst} = \frac{1}{4\pi|\boldsymbol{x}|}e^{-|\boldsymbol{x}|/\ell_d}. \quad (36)$$

The average potential conditional on the nearest particle is screened.

Taking the divergence of (32), using (33), noting $\nabla P_{s,nst}(\boldsymbol{x},\boldsymbol{r}) = \boldsymbol{0}$ for a homogeneous system, one finds

$$\varepsilon\nabla\cdot\langle \boldsymbol{E}\rangle(\boldsymbol{x}) = \sum_{k=1}^{N} q_k n^k(\boldsymbol{x}), \quad (37)$$

where

$$n^k(\boldsymbol{x}) = \int n^k_{s,nst}(\boldsymbol{x},\boldsymbol{r}) P_{s,nst}(\boldsymbol{x},\boldsymbol{r}) d^3r, \quad (38)$$

is the number density of species k particles. Using the Boltzmann distribution similar to (34) with potential $\langle\phi\rangle$ for the average electric field ($\langle \boldsymbol{E}\rangle = -\nabla\langle\phi\rangle$), we find the Debye-Hückel equation for the ensemble average of the potential,

$$\nabla^2\langle\phi\rangle(\boldsymbol{x}) - \langle\phi\rangle(\boldsymbol{x})/\ell_d^2 = 0. \quad (39)$$

Under the assumptions of thermodynamic equilibrium and charge neutrality, both the ensemble averaged potential and the potential conditionally averaged on the nearest particle are screened with the Debye length ℓ_d. Relation (37) can also be obtained by directly integrating (60) over $\boldsymbol{r}$, resulting in relation [2.13] of Zhang and Prosperetti,[23] based on the original definition of the ensemble average. The fact that we can obtain it both ways confirms the consistency between the nearest particle statistics introduced here and the original ensemble average.

This example shows that, as a mathematical tool, the nearest particle statistics can be used to obtain the Debye screening effect, while the ultimate reason for existence of the Debye length ℓ_d is the physics of thermodynamic equilibrium and charge neutrality.

Similar to this system of charged particles, by studying the averaged equation for the average velocity conditional on the nearest particle, one can also obtain the Brinkman screening for a Stokes flow passing a dilute array of fixed particles.

B. Disperse multiphase flows

We now use this method to study a more difficult problem, the momentum exchange in a two-phase flow. For disperse multiphase flows, the continuous phase is always described using the Eulerian method. Both Lagrangian and Eulerian methods have been employed to describe the disperse phase.[7,16,24–27] The drag and the added mass force are the best known phase interaction forces in multiphase flows. Although volume fraction dependent force models have been used[28–30] to calculate these forces, the effects of particle distributions and spatial gradients, with the exception for the lift force, have not been systematically considered in force models. Multiphase flow theory with such force models alone are known to be insufficient and inconsistent.[27,31] For instance, the well-known concept of the effective viscosity cannot be obtained from models containing only these forces. Furthermore, such models are not hyperbolic,[32,33] causing numerical results to diverge as the mesh refines in numerical calculations.[34,35] Detailed studies[12,15,23,36,37] show that there is a system of important stresses or momentum fluxes. The hyperbolicity is related to these stresses.[32,37] The phase interaction represented by the PFP stress studied in this work belongs to the category often called the three-way couplings resulting from particle-particle interactions mediated by the fluid.[31]

To consider such couplings in a Lagrangian description of the disperse phase, the phase interaction force needs to be sensitive to the positions of many surrounding particles.[27] In an Eulerian description, since the force is not for an individual particle, it should be a function of the probability distribution of the surrounding particles. From this point of view, the force model for an Eulerian-Eulerian description should be easier to achieve than the forces models in an Eulerian-Lagrangian description. The PFP stress defined in (22) can be considered as a correlation between the phase interaction forces and relative particle positions, containing the information of the particle distribution. The forces on the particles come from several physical origins, as for the drag, added mass force, and the Basset force. One can use definition (22) to study the corresponding stresses from these forces. In the following, as the first example in the multiphase flow, we choose to study the stress corresponding to the Stokes drag to gain insights of the physical meanings and mathematical properties. As pointed out by one of the reviewers, the most impactful application of this method will be the numerical calculation of the PFP stress using particle-resolved simulations. The examples provided here only serve the purpose of establishing the concept of this PFP stress and to understand its basic properties.

For a statistically uniform and isotropic particle distribution in a Stokes flow, the average force on the particle at $\boldsymbol{x}$ with the nearest particle at distance $\boldsymbol{r}$ away can be written as

$$\overline{\boldsymbol{f}}_{nst}(\boldsymbol{x},\boldsymbol{y}) = \boldsymbol{A}(\theta_p,\boldsymbol{r})\cdot\boldsymbol{v}_r(\boldsymbol{x}) + \boldsymbol{B}(\theta_p,\boldsymbol{r})\cdot\boldsymbol{v}_r(\boldsymbol{y}), \quad (40)$$

where $\boldsymbol{A}$ and $\boldsymbol{B}$ are the resistance tensors[38] even in variable $\boldsymbol{r}$, and $\boldsymbol{v}_r(\boldsymbol{x})$ and $\boldsymbol{v}_r(\boldsymbol{y})$ are the average relative velocities between the particle and the fluid phases at locations $\boldsymbol{x}$ and $\boldsymbol{y}=\boldsymbol{x}+\boldsymbol{r}$. Near $\boldsymbol{x}$, we can write

$$\boldsymbol{v}_r(\boldsymbol{y}) = \boldsymbol{v}_r(\boldsymbol{x}) + \boldsymbol{r}\cdot\nabla\boldsymbol{v}_r(\boldsymbol{x}) + \frac{\boldsymbol{r}\boldsymbol{r}}{2}:\nabla\nabla\boldsymbol{v}_r(\boldsymbol{x}) + O(\ell_p/L)^3. \quad (41)$$

Substituting (41) into (40) and then into (22), (23) and (25), with an error of $O(\ell_p/L)^3$, we find

$$\begin{aligned}\theta_p(\boldsymbol{x})\boldsymbol{\Sigma}_{pfp}(\boldsymbol{x}) &= \frac{1}{2}\int \boldsymbol{r}\overline{\boldsymbol{f}}_{nst}\overline{h}_2 P_2 d^3r \\ &= \frac{1}{2}\int \boldsymbol{r}\boldsymbol{B}(\theta_p,\boldsymbol{r})\boldsymbol{r}\overline{h}_2 P_2 d^3r : \nabla\boldsymbol{v}_r(\boldsymbol{x}), \quad (42)\end{aligned}$$

and

$$n_p\boldsymbol{f}_\ell = \int [\boldsymbol{A}(\theta_p,\boldsymbol{r}) + \boldsymbol{B}(\theta_p,\boldsymbol{r})]\cdot\boldsymbol{v}_r(\boldsymbol{x})\overline{h}_2 P_2 d^3r. \quad (43)$$

In this force the terms involving $\nabla\nabla\boldsymbol{v}_r(\boldsymbol{x})$ are canceled by the pseudo-stress in (25). The last integral in (42) is a fourth order with the dimension of viscosity.

For the leading order in the particle volume fraction θ_p, the effect of the particle interaction can be studied by considering a pair of particles with radii a in a pure fluid, because the probability of having a third particle nearby is of order θ_p^3 and negligible. In this case, the resistance tensors can be approximated as

$$\boldsymbol{A}(0,\boldsymbol{r}) = -6\pi\mu a\boldsymbol{I}, \ \boldsymbol{B}(0,\boldsymbol{r}) = 6\pi\mu\, a\,\frac{3a}{4r}\Big(\boldsymbol{I} + \frac{\boldsymbol{r}}{r}\frac{\boldsymbol{r}}{r}\Big). \quad (44)$$

These are only the leading order (in a/r) approximations and can be used to obtain the leading order approximation in θ_p for the local force $\boldsymbol{f}_\ell$ and the PFP stress. With higher order terms (in a/r), and considering the fluid velocity induced by particle motions, one

can also use the method described in this work to obtain the first order approximation of drag in the particle volume fraction. However, that study is beyond the scope of this work and will be reported elsewhere. Using[15,18,19] $\overline{h}_2 \approx \exp[-4\pi n_p(r^3-(2a)^3)/3]$ and $P_2 \approx n_p^2$, one finds $\boldsymbol{f}_\ell \approx -6\pi\mu a\boldsymbol{v}_r$, and

$$\theta_p\boldsymbol{\Sigma}_{pfp} \approx \mu_{pfp}\left\{(\nabla\overline{\boldsymbol{v}}_r)^T + \frac{1}{5}\Big[\nabla\cdot\overline{\boldsymbol{v}}_r\boldsymbol{I} + \nabla\overline{\boldsymbol{v}}_r + (\nabla\overline{\boldsymbol{v}}_r)^T\Big]\right\}, \quad (45)$$

where

$$\mu_{pfp} = \frac{9}{16}\Gamma(4/3)\theta_p^{2/3}\mu, \quad (46)$$

is the PFP viscosity with μ being the fluid viscosity and $\Gamma(\cdot)$ being the Γ-function. This PFP viscosity should not be confused with the effective viscosity for a particle suspension. The PFP stress associated with this viscosity is a term in the phase interaction force density in (24) that appears in the averaged momentum equations for the fluid and particle phases in equal magnitudes but opposite signs. By summing these two momentum equations to obtain the mixture momentum equation, the force densities, including the PFP stress terms, cancel, while the effective viscosity is a concept for the mixture.[15,23]

As another example of the disperse two-phase flow, we study a steady uniform potential flow. In this case, the force $\overline{\boldsymbol{f}}_{nst}$ is a function of the relative velocity $\overline{\boldsymbol{v}}_r$ between the phases. We can then write $\overline{\boldsymbol{f}}_{nst} = \boldsymbol{f}(\overline{\boldsymbol{v}}_r, \boldsymbol{r})$. If we now reverse both the relative velocity $\overline{\boldsymbol{v}}_r$ and the relative particle position $\boldsymbol{r}$, by spatial symmetry, we have $\boldsymbol{f}(\overline{\boldsymbol{v}}_r, \boldsymbol{r}) = -\boldsymbol{f}(-\overline{\boldsymbol{v}}_r, -\boldsymbol{r})$. This relation can also be obtained by rotation of the coordinates. Let S be a plane containing both vectors $\overline{\boldsymbol{v}}_r$ and $\boldsymbol{r}$, and $\hat{\boldsymbol{s}}$ be the unit normal of S. The above identity can be obtained by 180° rotation about $\hat{\boldsymbol{s}}$. Furthermore, for potential flows, when the velocity is reversed, the force remains unchanged, or $\boldsymbol{f}(-\overline{\boldsymbol{v}}_r, -\boldsymbol{r}) = \boldsymbol{f}(\overline{\boldsymbol{v}}_r, -\boldsymbol{r})$. Using these relations, we have

$$\begin{aligned}\overline{\boldsymbol{f}}_{nst}(\boldsymbol{r}) = \boldsymbol{f}(\overline{\boldsymbol{v}}_r, \boldsymbol{r}) &= -\boldsymbol{f}(-\overline{\boldsymbol{v}}_r, -\boldsymbol{r}) \\ &= -\boldsymbol{f}(\overline{\boldsymbol{v}}_r, -\boldsymbol{r}) = -\overline{\boldsymbol{f}}_{nst}(-\boldsymbol{r}). \quad (47)\end{aligned}$$

With this relation, $P_2(\boldsymbol{x}, \boldsymbol{x}+\boldsymbol{r}) = P_2(\boldsymbol{x}+\boldsymbol{r}, \boldsymbol{x})$, and definitions (18) and (23), we find $\boldsymbol{f}_o = \boldsymbol{0}$ and $\boldsymbol{T} = \boldsymbol{0}$ for potential flows with uniform relative phase velocities and uniform and isotropic particle distributions. As a direct consequence of this, the local phase interaction force $\boldsymbol{f}_\ell = \boldsymbol{0}$. In a potential flow, since force $\overline{\boldsymbol{f}}_{nst}$ is proportional to the square of the relative velocity between the phases, the stress must then be a tensor also proportional to the velocity squared. The only such tensor with the correct dimension possible is

$$\theta_p\boldsymbol{\Sigma}_{pfp} = \rho_f[C_1(\theta_p)(\overline{\boldsymbol{v}}_r\cdot\overline{\boldsymbol{v}}_r)\boldsymbol{I} + C_2(\theta_p)\overline{\boldsymbol{v}}_r\overline{\boldsymbol{v}}_r], \quad (48)$$

where ρ_f is the fluid density, C_1 and C_2 are the coefficients depending on the particle volume fraction to be determined numerically.

This example shows importance of the PFP stress. Suppose one has numerical simulations of potential flows using periodic domain for uniform particle distributions and then uses the numerical results to calculate the phase interaction force and finds that the result is zero. Without the concept of the PFP stress, one would conclude that in a potential flow the presence of particles has no effect on the averaged momentum equations, which is correct in cases of uniform systems, but not so for non-uniform cases. The PFP stress (48) represents the Bernoulli effect. For a cloud of particles, with the volume fraction gradient near the edge, the gradient of the PFP stress attracts particles into the cloud and repels the fluid phase. Furthermore, the PFP stress is not isotropic causing the deformation of the cloud.

V. DISCUSSIONS AND CONCLUSIONS

For a uniform system, as in most of today's numerical simulations, the PFP stress can be calculated as follows. Let N_{en} be the number of numerical simulations performed. By replacing $\int(\cdot)P(\mathscr{C})d\mathscr{C}$ with $\lim_{N_{en}\to\infty}\frac{1}{N_{en}}\sum_{\mathscr{C}=1}^{N_{en}}(\cdot)$ in (7) according to the definition of ensemble average, the volume average of the stress can be calculated as

$$\boldsymbol{\Sigma}_{pfp} = \lim_{N_{en}\to\infty}\frac{1}{N_{en}}\sum_{\mathscr{C}=1}^{N_{en}}\boldsymbol{\Sigma}_{pfp}^{\mathscr{C}}, \quad (49)$$

where

$$\boldsymbol{\Sigma}_{pfp}^{\mathscr{C}} = \frac{1}{2V_p}\sum_{i=1}^{N_p}\frac{1}{N_i}\sum_{j_i=1}^{N_i}(\boldsymbol{\xi}_{j_i} - \boldsymbol{\xi}_i)\boldsymbol{f}_i, \quad (50)$$

is the volume averaged stress in configuration $\mathscr{C}$, with V_p being the total particle volume in the configuration, N_p the number of particles in $\mathscr{C}$, N_i the number of the nearest particles of particle i, $\boldsymbol{f}_i$ the particle-field interaction force on particle i, $\boldsymbol{\xi}_i$ the position of particle i, and $\boldsymbol{\xi}_{j_i}$ the position of the j_i-th nearest particle to particle i. In most of the cases with moving (or randomly placed) particles, each particle will have one nearest neighbor ($N_i = 1$). Furthermore, for steady flows, time averaging can also be performed to enhance the convergence.

Since calculations of the local force and the PFP stress are based on the nearest particle probability, which decays rapidly at far field, one can also perform simulations with local gradients in a periodic domain to study effects of gradients in the particulate system. If the length scale associated with the gradient is much

greater than the inter-particle distance and smaller than the size of the computational domain, the force and the stress models developed based on such simulations are then valid for general system.

In conclusion, instead of providing a new numerical method to simulate long-range particle interactions, in this work the difficulty associated with mathematical analysis of long-range particle interaction is bypassed by establishing the relation between the ensemble average and the average conditional on the nearest neighbor. Using this relation, a particle-fluid-particle or particle-field-particle (PFP) stress is defined. By decomposing the particle-field interaction force into the local force $\boldsymbol{f}_\ell$ and the divergence of the PFP stress, one can extract additional physics from numerical results to develop models for statistically heterogeneous particulate systems.

ACKNOWLEDGMENT

Author is grateful for many in-depth discussions with Dr. Rick Rauenzahn and Dr. Jiajia Waters of Los Alamos and Prof. Sivaramakrishnan Balachandar of University of Florida. The financial support is provided by the Advanced Simulation and Computing (ASC) program under the auspices of the United States Department of Energy.

APPENDIX – AVERAGE FOR THE CONTINUOUS PHASE

In Section 2, for particle quantities, we have derived the relation between the ensemble average and the average conditional on the nearest particle. In this Appendix, we extend the derivation to the quantities pertaining to the continuous phase. Similar to (4), for a position $\boldsymbol{x}$ we define

$$h_i(\boldsymbol{x},\mathscr{C}) = \frac{1}{N_x(\boldsymbol{x},\mathscr{C})}\prod_j H(|\boldsymbol{\xi}_j-\boldsymbol{x}|-|\boldsymbol{\xi}_i-\boldsymbol{x}|). \quad (51)$$

where H is the Heaviside function (with the convention $H(0)=1$), and

$$N_x(\boldsymbol{x},\mathscr{C}) = \sum_i\prod_j H(|\boldsymbol{\xi}_j-\boldsymbol{x}|-|\boldsymbol{\xi}_i-\boldsymbol{x}|)\geq 1, \quad (52)$$

is the number of the nearest particles to position $\boldsymbol{x}$.

Using the property of the δ-function, for any configuration $\mathscr{C}$ and position $\boldsymbol{x}$, we have

$$\int\sum_i h_i(\boldsymbol{x},\mathscr{C})\delta(\boldsymbol{\xi}_i-\boldsymbol{y})d^3y = \sum_i h_i(\boldsymbol{x},\mathscr{C}) = 1. \quad (53)$$

The volume fraction of the continuous phase is[12,16]

$$\theta_c(\boldsymbol{x}) = \int \chi_c(\boldsymbol{x},\mathscr{C})P(\mathscr{C})d\mathscr{C}, \quad (54)$$

where χ_c is the phase indicator function defined as: $\chi_c(\boldsymbol{x},\mathscr{C})=1$, if $\boldsymbol{x}$ is in the continuous phase in configuration $\mathscr{C}$, and $\chi_c(\boldsymbol{x},\mathscr{C})=0$, otherwise. For a generic continuous phase quantity $q_c(\boldsymbol{x},\mathscr{C})$ at position $\boldsymbol{x}$, its ensemble average is defined as[12,16]

$$\langle q_c\rangle(\boldsymbol{x}) = \frac{1}{\theta_c(\boldsymbol{x})}\int \chi_c(\boldsymbol{x},\mathscr{C})q_c(\boldsymbol{x},\mathscr{C})P(\mathscr{C})d\mathscr{C}. \quad (55)$$

Multiplying the left-hand side of (53) to the right-hand side of (55) and then exchanging the orders of the integrations, similar to (6) one finds

$$\langle q_c\rangle(\boldsymbol{x}) = \int\langle q_c\rangle_{nst}(\boldsymbol{x},\boldsymbol{y})P^c_{nst}(\boldsymbol{y}|\boldsymbol{x})d^3y, \quad (56)$$

where

$$\langle q_c\rangle_{nst}(\boldsymbol{x},\boldsymbol{y}) = \frac{1}{\theta_c(\boldsymbol{x})P^c_{nst}(\boldsymbol{y}|\boldsymbol{x})}\int q_c(\boldsymbol{x},\mathscr{C})\chi_c(\boldsymbol{x},\mathscr{C}) \sum_i h_i(\boldsymbol{x},\mathscr{F})\delta(\boldsymbol{\xi}_i-\boldsymbol{y})P(\mathscr{C})d\mathscr{C}, \quad (57)$$

is the average of the continuous phase quantity q_c at $\boldsymbol{x}$ under the condition that position $\boldsymbol{x}$ is in the continuous phase, while position $\boldsymbol{y}$ is occupied by the center of the nearest particle.

$$P^c_{nst}(\boldsymbol{y}|\boldsymbol{x}) = \frac{1}{\theta_c(\boldsymbol{x})}\int \chi_c(\boldsymbol{x},\mathscr{C}) \sum_{i=1} h_i(\boldsymbol{x},\mathscr{F})\delta(\boldsymbol{\xi}_i-\boldsymbol{y})P(\mathscr{C})d\mathscr{C}, \quad (58)$$

is the probability density of finding the nearest particle to $\boldsymbol{x}$ at $\boldsymbol{y}$ conditional on $\boldsymbol{x}$ being a point in the continuous phase. Using (53) and (54), one finds that this probability density normalizes to

$$\int P^c_{nst}(\boldsymbol{y}|\boldsymbol{x})d^3y = 1. \quad (59)$$

For a constant $\boldsymbol{r}$, the gradient of $\langle q_c\rangle_{nst}(\boldsymbol{x},\boldsymbol{x}+\boldsymbol{r})$ can be calculated as

$$\begin{aligned}
&\theta_c(\boldsymbol{x})P^c_{nst}(\boldsymbol{x}+\boldsymbol{r}|\boldsymbol{x})\nabla\langle q_c\rangle_{nst}(\boldsymbol{x},\boldsymbol{x}+\boldsymbol{r})\\
=&\theta_c(\boldsymbol{x})P^c_{nst}(\boldsymbol{x}+\boldsymbol{r}|\boldsymbol{x})\langle\nabla q_c\rangle(\boldsymbol{x},\boldsymbol{x}+\boldsymbol{r})\\
+&[\langle q_c\rangle(\boldsymbol{x})-\langle q_c\rangle_{nst}(\boldsymbol{x},\boldsymbol{x}+\boldsymbol{r})]\nabla[\theta_c(\boldsymbol{x})P^c_{nst}(\boldsymbol{x}+\boldsymbol{r}|\boldsymbol{x})]\\
+&\int[q_c(\boldsymbol{x},\mathscr{F})-\langle q_c\rangle(\boldsymbol{x})]\sum_i h_i(\boldsymbol{x},\mathscr{F})\delta(\boldsymbol{\xi}_i-\boldsymbol{x}-\boldsymbol{r})\\
&\nabla\chi_c(\boldsymbol{x},\mathscr{C})P(\mathscr{C})d\mathscr{C}\\
+&\int[q_c(\boldsymbol{x},\mathscr{F})-\langle q_c\rangle(\boldsymbol{x})]\chi_c(\boldsymbol{x},\mathscr{C})\\
&\sum_i\nabla[h_i(\boldsymbol{x},\mathscr{C})\delta(\boldsymbol{\xi}_i-\boldsymbol{x}-\boldsymbol{r})]P(\mathscr{C})d\mathscr{C}, \quad (60)
\end{aligned}$$

in which

$$\nabla[h_i(\boldsymbol{x},\mathscr{F})\delta(\boldsymbol{\xi}_i-\boldsymbol{x}-\boldsymbol{r})]=\delta(\boldsymbol{\xi}_i-\boldsymbol{x}-\boldsymbol{r})\sum_k(\hat{\boldsymbol{r}}-\hat{\boldsymbol{r}}_k)\delta(r_k-r)\prod_{j\neq k}H(r_j-r), \quad (61)$$

with $\boldsymbol{r}_k=\boldsymbol{\xi}_k-\boldsymbol{x}$, $\hat{\boldsymbol{r}}=\boldsymbol{r}/r$ and $\hat{\boldsymbol{r}}_k=\boldsymbol{r}_k/r_k$. Noting that in (61), the term with $k=i$ contributes nothing because $\boldsymbol{r}_i=\boldsymbol{r}$. For (61) to be nonzero, a particle other than the one with index i (at $\boldsymbol{x}+\boldsymbol{r}$) has to be at the distance $r=|\boldsymbol{r}|$ away from $\boldsymbol{x}$; therefore, the last term in (60) is caused by multi-particle interactions.

[1] J. A. Rackers, C. Liu, P. Ren, and J. W. Ponder, "A physically grounded damped dispersion model with particle mesh Ewald summation," The Journal of Chemical Physics **149**, 084115 (2018), https://doi.org/10.1063/1.5030434.

[2] F. Nestler, M. Pippig, and D. Pott, "Fast Ewald summation based on NFFT with mixed periodicity," The Journal of Computational Physics **285**, 280–315 (2015).

[3] Y. Yao and J. Capecelatro, "Competition between drag and coulomb interactions in turbulent particle-laden flows using a coupled-fluid-Ewald-summation based approach," Phys. Rev. Fluids **3**, 034301 (2018).

[4] M. P. Allen and D. J. Tildesley, *Computer Similation of Liquids* (Oxford University Press, 198 Madisn Avenue, New York, 2017).

[5] H. Tavassoli, E. Peters, and J. Kuipers, "Direct numerical simulation of fluid-particle heat transfer in fixed random arrays of non-spherical particles," Chemical Engineering Science **129**, 42 – 48 (2015).

[6] L. Wang, C. Peng, Z. Guo, and Z. Yu, "Lattice boltzmann simulation of particle-laden turbulent channel flow," Computers and Fluids **124**, 226 – 236 (2016).

[7] G. Akiki and S. Balachandar, "Immersed boundary method with non-uniform distribution of lagrangian markers for a non-uniform eulerian mesh," Journal of Computational Physics **307**, 34–59 (2016).

[8] D. L. Koch, R. J. Hill, and A. S. Sangani, "Brinkman screening and the covariance of the fluid velocity in fixed beds," Physics of Fluids **10**, 3035–3037 (1998), https://doi.org/10.1063/1.869830.

[9] D. C. Brydges and P. A. Martin, "Coulomb systems at low density: A review," Journal of Statistical Physics **96**, 1163–1330 (1999).

[10] P. Hertz, "Über den gegenseitigen durchschnittlichen abstand von punkten, die mit bekannter mittlerer dichte im raume angeordnet sind," Math. Ann. **67**, 387–398 (1909).

[11] J. H. Irving and I. G. Kirkwood, "The statistical theory of transport processes. IV. The equations of hydrodynamics," J. Chem. Phys. **18**, 817–829 (1950).

[12] D. Z. Zhang and A. Prosperetti, "Averaged equations for inviscid disperse two-phase flow." J. Fluid Mech. **267**, 185–219 (1994).

[13] D. Z. Zhang and R. M. Rauenzahn, "A viscoelastic model for dense granular flows," Journal of Rheology **41**, 1275–1298 (1997), https://doi.org/10.1122/1.550844.

[14] D. Z. Zhang, X. Ma, and R. M. Rauenzahn, "Interspecies stress in momentum equations for dense binary particulate systems," Phys. Rev. Lett. **97**, 048301 (2006).

[15] G. K. Batchelor, "The stress system in a suspension of force-free particles," J. Fluid Mech. **41**, 545–570 (1970).

[16] D. Z. Zhang, W. B. VanderHeyden, Q. Zou, and N. T. Padial-Collins, "Pressure calculations in disperse and continuous multiphase flows." Int. J. Multiphase Flow **33**, 86–100 (2007).

[17] S. Chandrasekhar, "Stochastic problems in physics and astronomy," Reviews of Modern Physics **15**, 1 – 89 (1943).

[18] S. Torquato, "Random heterogeneous media: Microstructure and improved bounds on effective properties," Appl. Mech. Rev. **44**, 37 – 76 (1991).

[19] S. Torquato, B. Lu, and J. Rubinstein, "Nearest-neighbor distribution functions in many-body systems," Phys. Rev. A **41**, 2059–2075 (1990).

[20] E. J. Hinch, "An averaged-equation approach to particle interactions in fluid suspension," J. Fluid Mech. **83**, 695 – 720 (1977).

[21] A. Prosperetti and A. Jones, "Pressure forces in disperse two-phase flow," International Journal of Multiphase Flow **10**, 425 – 440 (1984).

[22] D. A. McQuarrie, *Statistical mechancis* (Happer & Row, 10 East 53rd Street, New York, 1976).

[23] D. Z. Zhang and A. Prosperetti, "Momentum and energy equations for disperse two-phase flows and their closure for dilute suspensions." Int. J. Multiphase Flow **23**, 425–453 (1997).

[24] D. Drew and S. L. Passman, *The theory of multicomponent fluids* (Springer, New York, 1998).

[25] N.A.Patankar and D.D.Joseph, "Modeling and numerical simulation of particulate flows by the eulerian-lagrangian approach," International Journal of Multiphase Flow **27**, 1659–1684 (2001).

[26] S. Balachandar and J. K. Eaton, "Turbulent dispersed multiphase flow," Annual Review of Fluid Mechanics **42**, 111–133 (2010).

[27] G. Akiki, W. Moore, and S. Balachandar, "Pairwise-interaction extended point-particle model for particle-laden flows," Journal of Computational Physics **351**, 329 – 357 (2017).

[28] J. F. Richardson and W. N. Zaki, "Sedimentation and fluidisation: part i," Trans. Inst. Chem. Engrs., **34**, 35–53 (1954).

[29] S. Ergun, "Fluid flow through packed columns," Chem. Eng. Prog. **48**, 89–94 (1952).

[30] L. van Wijngaarden, "Hydrodynamic interaction between gas bubbles in liquid," J. Fluid Mech. **77**, 27– 44 (1976).

[31] R. O. Fox, "Large-eddy-simulation tools for multiphase flows," Annual Review of Fluid Mechanics **44**, 47–76 (2012).

[32] D. Lhuillier, C. H. Chang, and T. G. Theofanous, "On the quest for a hyperbolic effective- field model of disperse flows." J. Fluid Mech. **731**, 184–194 (2013).

[33] T. Vazquez-Gonzalez, A. Llor, and C. Fochesato, "Ransom test results from various two-fluid schemes: Is enforcing hyperbolicity a thermodynamically consistent option?" International Journal of Multiphase Flow **81**, 104 – 112 (2016).

[34] M. Ndjinga, "Influence of interfacial pressure on the hyperbolicity of the two-fluid model," C. R. Acad. Sci. Paris **344**, 407–412 (2007).

[35] T. G. Theofanous and C. H. Chang, "Shock dispersal of dilute particle clouds." J. Fluid Mech. **841**, 732–745 (2018).

[36] B. Kong, R. O. Fox, H. Feng, J. Capecelatro, R. Patel, O. Desjardins, and R. O. Fox, "Euler-euler anisotropic gaussian mesoscale simulation of homogeneous cluster-induced gas-particle turbulence," AIChE Journal **63**, 2630–2643 (2017).

[37] R. O. Fox, "A kinetic-based hyperbolic two-fluid model for binary hard-sphere mixtures," J. Fluid Mech. **877**, 282–329 (2019).

[38] J. F. Brady and G. Bossis, "Stokesian dynamics," Ann. Rev. Fluid Mech. **20**, 111 – 157 (1988).